Improved vortex lattice method for drag prediction of supersonic wings using shock cone modelling

Hemant Joshi[1*], Peter Thomas[2], Christabel Tan[3], Hongwei Wu[4]

[1,2,3,4*]Center of Engineering Research, University of Hertfordshire, College Lane, Hatfield, AL10 9AB, Hertfordshire, United Kingdom.

*Corresponding author(s). E-mail(s): h.joshi3@herts.ac.uk;
Contributing authors: p.thomas5@herts.ac.uk; c.k.l.tan@herts.ac.uk; h.wu6@herts.ac.uk;

Abstract

Drag prediction in supersonic wing design is a computationally demanding task due to complex flow physics and the high volume of data required for accurate modelling. High-fidelity CFD methods, while precise, are often too resource intensive for iterative early-stage design. This study presents a reduced-order approach that enhances the conventional Vortex Lattice Method (VLM) by incorporating the Taylor-Maccoll hypervelocity method (TMHM) to model shock cones and estimate wave and pressure drag due to compressibility effects, but does not model viscous skin friction drag explicitly. The resulting solver offers a balance between computational efficiency and predictive accuracy, enabling rapid analysis across a wide range of supersonic configurations. Validation against experimental and SST RANS data for Mach numbers from 1.0 to 2.7 shows an improvement of up to 20% in drag prediction over standard VLM, with an accuracy ranging from 90% to 95% for various wing geometries including delta, dihedral, and highly swept designs. This method supports the development of data-efficient, fast turnaround tools for the design of next-generation supersonic aircraft.

Keywords: Supersonic Vortex Lattice Method, Shockcone, Drag Prediction, Supersonic Drag

Nomenclature

a = Local speed of the sound

C_d	=	Coefficient of drag
C_p	=	Coefficient of pressure
c	=	Chord length of an aerofoil
CFD	=	Computational fluid dynamics
CPU	=	Central processing unit
dt	=	Time-step
i	=	number of partition of the wing
ISA	=	International Standards of Atmosphere
β	=	Shock angle
γ	=	Specific heat ratio
θ	=	Circumferential coordinate
θ_s	=	Half cone angle
μ	=	Prandtl Meyer function
ρ	=	Density
LOM	=	Low-order modelling
l	=	length of the shock
M	=	Free-stream Mach number
Pb	=	Pressure acting on the base cone
Pc	=	Pressure acting on the shock cone
RANS	=	Reynolds Average Navier Stokes
RAM	=	Random access memory
SVLM	=	Supersonic VLM
SST	=	Shear Stress Turbulence Method
TM	=	Taylor Maccoll
TMHM	=	Taylor Maccoll Hypervelocity Method
U	=	Speed of flow
u	=	Radial velocity on the Mach-cone
v	=	Velocity component in the direction of cone-angle
VLM	=	Vortex Lattice Method

1 Introduction

The design of supersonic aircrafts presents significant challenges due to the complex interplay between shock waves, boundary layer interactions, and rapidly evolving flow fields. Capturing these phenomena with high accuracy typically requires high-fidelity solvers based on the Navier–Stokes equations, such as Reynolds-averaged Navier-Stokes (RANS) models. However, these methods come at a substantial computational cost, making them impractical for large-scale parametric studies or early-stage design exploration [1, 2].

To address this, the aerospace community has long relied on low-order methods, such as potential flow solvers and VLM, valued for their efficiency and speed [3, 4]. These models have seen widespread use in subsonic and transonic analysis, but their application to supersonic flows remains limited. As the flow speed increases into the supersonic regime, the emergence of shock waves and associated wave drag introduces discontinuities that are poorly captured by conventional low-order formulations [5, 6].

This study helps to improve Taylor Maccoll's application in studying the velocity potential at high speeds [7, 8]. This study applies the classical Taylor–MacColl theory in a novel way to improve pressure coefficient prediction on supersonic panels within a modified VLM framework. The use of low-order solver and their hybrid with conventional high-order methods was explored to overcome the limitations associated with the low-order design approach [2, 9]. Some common use of these methods has been seen in studying the complex supersonic flow conditions of an aircraft undergoing shock cone formation [10]. Although supersonic VLM tools such as VORLAX exist [11], they typically do not explicitly model the local shock-cone pressure behaviour [12]. Our method improves the VLM by incorporating the shock-cone Cp correction using Taylor–MacColl theory.

In recent years, efforts have been made to enhance the predictive power of reduced-order models by integrating high-speed flow phenomena, particularly those related to shock interactions [13–17]. One promising direction involves the incorporation of shock cone modelling, traditionally derived from axisymmetric analytical solutions such as the Taylor-Maccoll equation [18, 19]. These methods provide insight into the conical shock structures that form around supersonic bodies [20] and have historically informed the design of waverider configurations and high-speed inlets [13, 21, 22].

Despite the value of these analytical tools, their integration into practical aerodynamic solvers remains limited. Conventional VLM, for instance, assumes incompressible irrotational flow and neglects the formation and propagation of shock waves. As a result, it tends to underestimate drag and mispredict aerodynamic loading under supersonic conditions [23, 24].

This presents a clear research gap: the need for a low-order modelling approach that retains the computational efficiency of VLM while incorporating physical corrections to account for shock-cone interactions. Recent studies have demonstrated the benefits of this hybrid model [25, 26], and have highlighted the importance of capturing shock wave effects for accurate prediction of performance in high-speed flows [27, 28].

This paper addresses this gap by proposing a modified low-order aerodynamic framework that couples VLM with conical shock interaction models. Each VLM panel is treated as an individual lifting surface that undergoes local shock cone formation, with pressure and velocity corrections derived from analytical solutions. This integration improves the ability of the model to predict waves and estimates pressure drag due to compressibility effects, but does not model viscous skin friction drag explicitly. offering improved accuracy while maintaining computational efficiency.

The proposed method serves as the basis for developing rapid physics-informed tools for the design of supersonic aircrafts, allowing fast evaluation of numerous configurations without the computational burden of high-fidelity simulations. This work advances the ability of low-order solvers to support conceptual and preliminary design processes in high-speed aerodynamics.

2 Methodology

This study develops a modified low-order aerodynamic model that incorporates conical shockwave effects into the VLM framework. Traditional VLM formulations, while

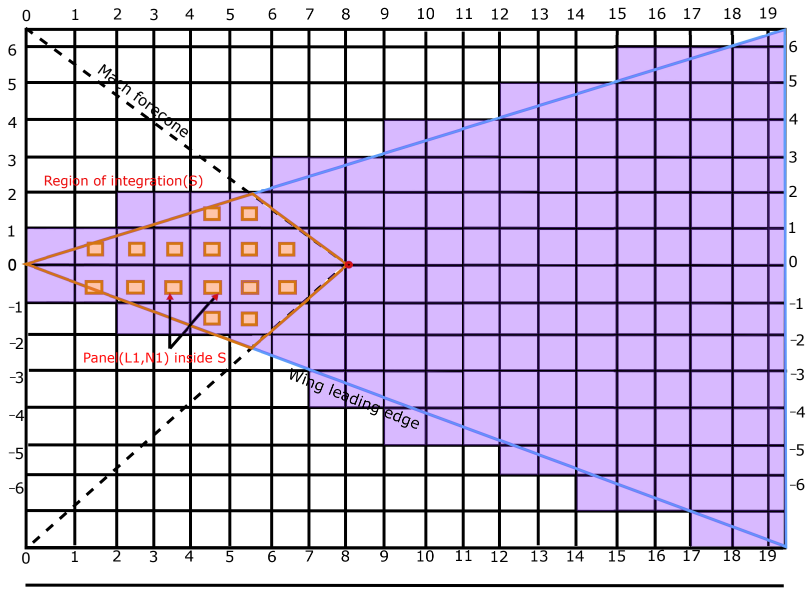

Fig. 1: Panel Representation of Flat Plate Delta Wings with Subsonic Leading Edge [30].

computationally efficient, do not account for the compressibility and wave phenomena inherent in supersonic flow regimes. To address this limitation, the proposed method introduces a *Mach-cone influence model* derived from conical shock theory, specifically tailored for integration with VLM panels.

The core of the approach lies in analytically modelling the local shock-cone structure that forms ahead of each VLM panel under supersonic conditions. Unlike conventional VLM applications, which assume incompressible and irrotational flow, this method incorporates the influence of Mach angle shifts and shock apex movement as part of the panel representation [29]. As supersonic speed increases, the Mach angle narrows, affecting the geometric interaction between the freestream and panel surface. This variation is captured through an adaptive adjustment in the placement of the panel and the location of the control point, leading to an improved prediction of local pressure gradients and force distributions.

Figure 1 illustrates the panelized representation of a flat delta wing, segmented into discrete control surfaces. In the supersonic regime, only panels within the Mach forecone contribute to the flow field at any given point, thereby reducing the domain of aerodynamic influence. This constraint is central to the proposed modelling framework, where the region of integration over the wing surface is dynamically determined by the Mach cone boundaries.

To model the conical shock structure, the Taylor-Maccoll equation is used, which describes axisymmetric flow over a pointed cone [31]. Although originally formulated for idealised conditions [18], its hypervelocity formulation [32] enables parametric estimation of velocity changes (u, v) across the shock front. These estimates are used to

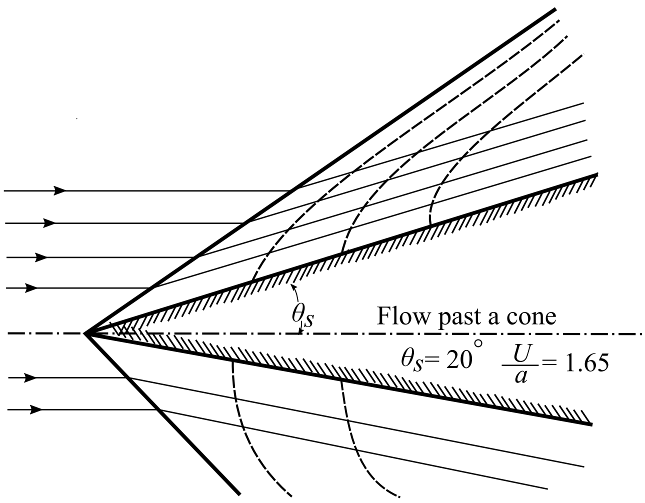

Fig. 2: Flow past the shock-cone [33].

correct for the local flow conditions perceived by each panel, thereby modifying the strength and orientation of the bound vortices in the VLM solution.

Figure 2 shows the characteristic shock cone flow field. The half angle θ_S defines the geometry of the conical surface, while the free-stream Mach number determines the inclination of the shock. This relationship guides the calculation of local panel influence, particularly in regions near sharp leading edges or slender forebodies. The method approximates a *single-cone forebody* model for each panel, treating each as a simplified shock generator that perturbs free-stream conditions within its influence zone.

The outcome of this integration is a hybrid solver that retains the computational speed of VLM but improves its fidelity in supersonic regimes by incorporating localised shock behaviour. This addresses a critical gap in low-order aerodynamic tools, which traditionally lack mechanisms to resolve shock-wave-induced forces. Moreover, by parametric linking shock geometry with panel location and flow conditions, the method supports design exploration for supersonic wings with varying sweep and leading-edge geometries.

2.1 Taylor-Maccoll Hypervelocity Framework for Supersonic Panels

The Taylor-Maccoll Hypervelocity Method (TMHM) provides an analytical approach to model high-speed flowfields around axisymmetric bodies, particularly cones, under supersonic and hypervelocity conditions. Originally developed for steady, inviscid, isentropic, and axisymmetric flow over cones assuming a calorically perfect gas [19], the method has since been extended to incorporate real gas effects including dissociation, ionisation, and excitation of internal energy modes in thermochemical non-equilibrium environments [32].

In this study, we used the Taylor-Maccoll method as a foundational tool to capture the formation and influence of shock cones on panels subjected to supersonic flow. While the classical Taylor–MacColl solution applies to axisymmetric flow around sharp cones, our modified TMHM formulation is adapted for panel-wise application on general lifting surfaces. This includes using the local Mach number and sweep angle to apply Cp corrections based on whether the panel lies within its Mach cone, thereby extending the utility of Taylor–MacColl theory to arbitrary wing geometries. Each panel on the lifting surface is modelled as a locally axisymmetric conical segment, allowing the application of TMHM to compute localised flow properties, radial and circumferential velocities, which are then coupled with the VLM for aerodynamic potential correction.

2.1.1 Simplified Taylor-Maccoll Formulation

The Taylor-Maccoll equation for axisymmetric supersonic flow is expressed as:

$$\left(1-\frac{v^2}{a^2}\right)\frac{\mathrm{d}^2u}{\mathrm{d}\theta^2}+(\cot\theta)\frac{\mathrm{d}u}{\mathrm{d}\theta}+\left(2-\frac{v^2}{a^2}\right)u=0 \tag{1}$$

Here, u and v are the radial and circumferential components of velocity, a is the local speed of sound, and θ is the angular coordinate. Under hypervelocity assumptions (i.e., $v \ll u$), the equation simplifies to:

$$\frac{\mathrm{d}^2u}{\mathrm{d}\theta^2}+\cot\theta\frac{\mathrm{d}u}{\mathrm{d}\theta}+2u=0 \tag{2}$$

Using the transformation $u(\theta)=f(\theta)\cos(\theta)$, this leads to a further simplification:

$$\frac{\mathrm{d}}{\mathrm{d}\theta}\left(\sin\theta\cos^2\theta\frac{\mathrm{df}}{\mathrm{d}\theta}\right)=0 \tag{3}$$

Solving this analytically yields the velocity components:

$$u(\theta)=A\left[1+\cos\theta\ln\left(\tan\frac{\theta}{2}\right)\right]+B\cos\theta \tag{4}$$

$$v(\theta)=A\left[\cot\theta-\sin\theta\ln\left(\tan\frac{\theta}{2}\right)\right]-B\sin\theta \tag{5}$$

The constants A and B are derived from the shock angle β, the upstream Mach number M, and the post-shock density ratio ρ, using:

$$u(\beta)=M\cos\beta \tag{6}$$

$$v(\beta)=-\frac{1}{\rho}M\sin\beta \tag{7}$$

with

$$\rho = \frac{(\gamma+1)M_1^2 \sin^2\beta}{(\gamma-1)M_1^2 \sin^2\beta + 2} \tag{8}$$

Solving the boundary conditions gives the following.

$$A = \left(1 - \frac{1}{\rho}\right) M \sin^2\beta \cos\beta \tag{9}$$

$$B = M - A\left(\frac{1}{\cos\beta} + \ln\tan\frac{\beta}{2}\right) \tag{10}$$

The normalised velocity expressions used in the VLM framework are thus:

$$\frac{u}{M} = \cos\theta + \left(1 - \frac{1}{\rho}\right)\sin^2\beta\cos\beta\left[1 - \frac{\cos\theta}{\cos\beta} + \cos\theta\ln\frac{\tan(\theta/2)}{\tan(\beta/2)}\right] \tag{11}$$

$$\frac{v}{M} = -\sin\theta + \left(1 - \frac{1}{\rho}\right)\sin^2\beta\cos\beta\left[\cot\theta + \frac{\sin\theta}{\cos\beta} - \sin\theta\ln\frac{\tan(\theta/2)}{\tan(\beta/2)}\right] \tag{12}$$

2.2 Integration with VLM for Shockcone Modelling

To incorporate supersonic effects into the Vortex Lattice Method, each panel is treated as generating its own localised Mach cone based on the free-stream Mach number and the surface geometry. This creates a panel-specific shock system that is used to modify local flow potentials as shown in Figure.3

2.2.1 Panel Discretization

The wing is discretised into a lattice of panels across chord-wise and span-wise directions:

$$\Delta x_j = \frac{c}{N_{chord}}, \quad j = 1, 2, ..., N_{chord} \tag{13}$$

$$\Delta y_i = \frac{b}{N_{span}}, \quad i = 1, 2, ..., N_{span} \tag{14}$$

The local shock cone of each panel is calculated by applying the TMHM-derived expressions to obtain velocity potentials based on the circumferential coordinate θ_i.

2.2.2 Velocity Potentials for Panels

Using the normalised TMHM expressions, the panel-level velocity components $u_i(\theta)$ and $v_i(\theta)$ are:

$$u_i(\theta) = \cos\theta + \left(1 - \frac{1}{\rho}\right)\sin^2\beta\cos\beta\left[1 - \frac{\cos\theta}{\cos\beta} + \cos\theta\ln\frac{\tan(\theta/2)}{\tan(\beta/2)}\right] \tag{15}$$

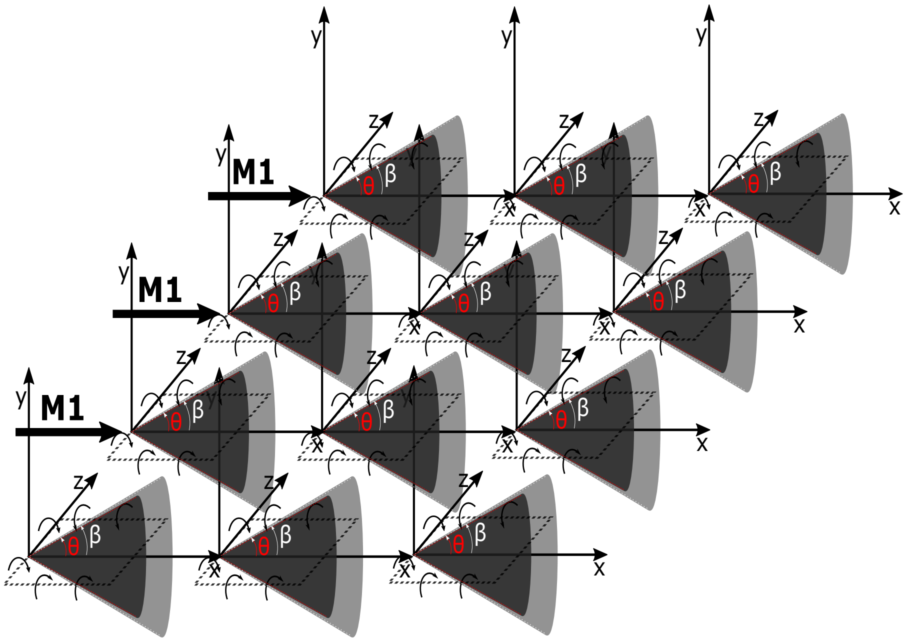

Fig. 3: Mach cone influence on each panel generalised using VLM.

$$v_i(\theta) = -\sin\theta + \left(1 - \frac{1}{\rho}\right)\sin^2\beta\cos\beta\left[\cot\theta + \frac{\sin\theta}{\cos\beta} - \sin\theta\ln\frac{\tan(\theta/2)}{\tan(\beta/2)}\right] \tag{16}$$

These expressions allow estimation of the flow potential around each panel. By assuming irrotational flow ($\partial v/\partial x = \partial u/\partial y$), the total velocity potential is derived as:

$$\Delta\Phi \approx \int_{panel} \phi_u(\theta)\, dS + \int_{panel} \phi_v(\theta)\, d\vec{S} \tag{17}$$

where $\phi_u(\theta) = \int u_i(\theta)\, d\theta$ and $\phi_v(\theta) = \int v_i(\theta)\, d\theta$, and dS, $d\vec{S}$ are scalar and vector differential area elements of the panel.

2.2.3 Shock Boundary Adjustments

At high Mach numbers, panels encounter local shock effects, especially near the leading edges. The shock-cone interaction modifies the boundary conditions at the location points (see Figure 5), affecting the vertical component of the velocity. These changes are implemented through corrected potential functions based on oblique shock theory and Rankine-Hugoniot conditions [34].

$$\phi'_u(\theta) = f(\phi_u(\theta), M, \beta) \tag{18}$$
$$\phi'_v(\theta) = f(\phi_v(\theta), M, \beta) \tag{19}$$

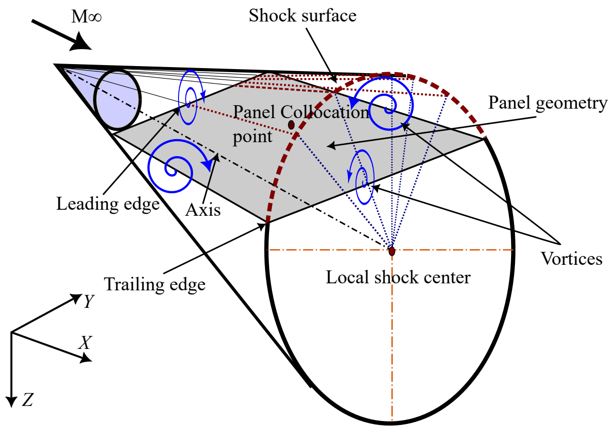

Fig. 4: Mach-cone over a panel geometry under shock surface.

$$\phi'_u(\theta) = f(\phi_u(\theta), M, \beta) \tag{20}$$

$$\phi'_v(\theta) = f(\phi_v(\theta), M, \beta) \tag{21}$$

where $\phi'_u(\theta)$ and $\phi'_v(\theta)$ are the adjusted potential components post-shock, M is the local Mach number, β is the shock angle and f represents the function that models the changes across the shock, based on the shock wave theory as shown in Fig.4.

$$P_2 = P_1 + \rho(M_1)^2(\sin(\beta)^2)\left(\frac{2}{\gamma+1} - \frac{1}{\rho}\right) \tag{22}$$

where P_1, ρ and M are the pressure, density and the Mach number of the freestream and β is the shock angle.

- **Superposition of panel contributions**
  The total potential ϕ and velocity V at any point in the field can be found by summing the contributions from all the panels. For a field point P, this can be

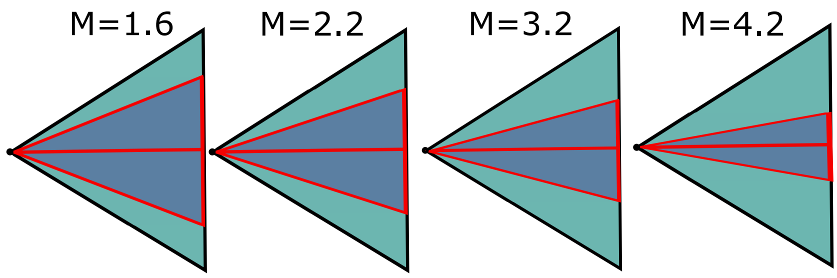

Fig. 5: Mach cone influence on the delta wing [3].

approximated as:

$$\Phi_P = \sum_{I=1}^{n} \Phi i \tag{23}$$

$$\nu_P = \sum_{i=1}^{n} \nu i \tag{24}$$

where n is the number of panels. The contributions from each panel (Φ_i, ν_i) are computed on the basis of the local $\phi_u i(\theta)$ and $\phi_v i(\theta)$ adjusted for the panel's orientation and observer's position.

- **Calculations for drag coefficient**
  The lift coefficient C_d can be calculated by integrating the pressure distribution across the lifting surface.

$$C_d = \frac{1}{S} \int_{surface} (P - P_\infty) dS. \sin(\alpha) \tag{25}$$

  where S is the reference area, P_∞ is the free-stream pressure and α is the angle of attack. The pressure P on each panel is calculated from the local flow properties determined by the new Shockcone modelling within VLM.

The novelty of the work lies in the development of a low-order hybrid aerodynamic framework that assigns a locally conical TMHM shock solution to each VLM panel. This allows the classical VLM to account for panel-specific supersonic flow behaviour, such as shock-cone interaction, oblique shock corrections, and local pressure recovery, without resorting to full CFD or Euler solvers. By computing the circumferential and radial velocity components for each panel through TMHM, and integrating these into the potential calculation of the vortex lattice, your method effectively enables shock-aware vortex strength estimation. Furthermore, using the shock angle (β), post-shock density ratio (ρ), and panel orientation, the model provides analytic corrections for the effects of flow turning and downwash.

3 Computational modelling

This work builds upon the Tornado framework, an open source VLM solver, which serves as the backbone for aerodynamic modelling. The tornado discretises lifting surfaces into a lattice of bound vortex filaments and applies linearised potential flow theory to solve for circulation distributions, thus computing aerodynamic forces and moments [35]. The present work extends the Tornado solver by integrating a novel Shockcone Modelling module that accounts for compressibility and shockwave effects in supersonic regimes through the Taylor-Maccoll hypervelocity method.

Figure 6 illustrates the architecture of the Tornado solver. The computational pipeline begins with user-defined geometry parameters and flight conditions, which are processed through Tornado's state initialisation routines. These routines call the International Standard Atmosphere (ISA) module to retrieve altitude-based environmental properties. The core Tornado VLM routines then perform aerodynamic calculations

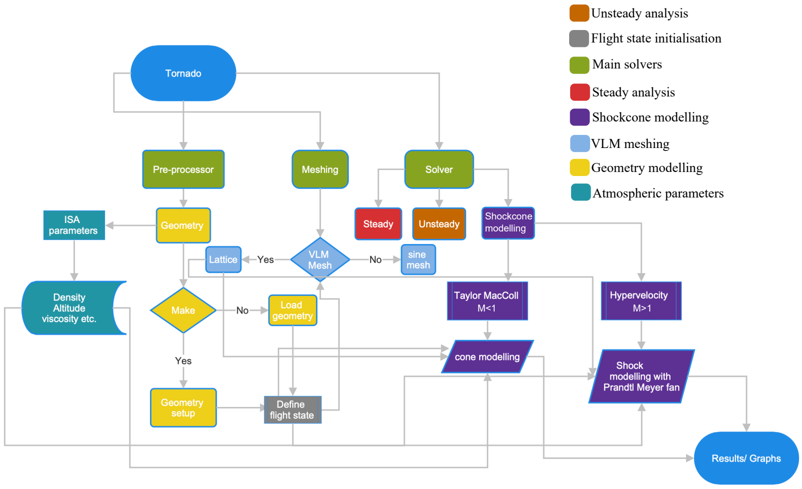

Fig. 6: Flowchart showing full Tornado architecture and the addition of the Shockcone modelling module.

under incompressible assumptions. To enable compressibility corrections, especially relevant for supersonic flows, a dedicated Shockcone Influence subroutine was incorporated within the Tornado framework. This routine, highlighted in Figure 7, is directly connected to the existing solution through Tornado's modular addfile system. It takes

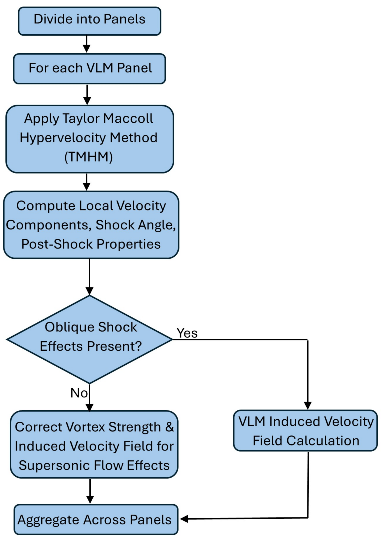

Fig. 7: Flowchart of Shockcone subroutine integrated within the Tornado solver.

user-specified values such as the cone half-angle (θ), freestream Mach number, and the specific heat ratio (γ), and performs several analytical steps to model flow changes due to shockwaves.

The routine begins by computing upstream flow properties from ISA, followed by calculating the Prandtl-Meyer function (μ) and the stagnation temperature in the free stream using isentropic flow relations [36]. These parameters are used to solve the oblique shock relations, yielding the post-shock Mach number and the pressure ratio across the conical surface. This modification enables the solver to estimate the pressure field more accurately by adjusting vortex influence terms within the VLM solver based on local compressibility effects.

Furthermore, to address applications in hypervelocity regimes, the Taylor-Maccoll method is implemented within a separate subroutine under the shockcone model. Here, the normal and tangential velocity components $u(\beta)$ and $v(\beta)$ are solved across the shock layer, specifically focussing on the cone surface, where the tangential component diminishes to zero. The variation of the velocity components (u/M and v/M) is evaluated in a range of cone angles to visualise the deviation from free-stream flow and the intensifying compressibility effects near the apex.

The results of these computations are stored in the Tornado output structure for post-processing and visualisation. This extended computational framework allows for a more accurate aerodynamic representation of supersonic and hypersonic flows by embedding compressibility and shockwave effects directly into the VLM formulation.

4 Modelling verification and validation

To establish the validity of the developed Shockcone solver, a comparative analysis was performed against established numerical solutions of the Taylor-Maccoll model of Ishimatsu [32]. The primary objective of this validation is to confirm the solver's ability to accurately capture shockwave-induced flow variations, particularly in the tangential and normal velocity components of the conical surface.

4.1 Axisymmetric Validation (Taylor–MacColl)

The validation was performed over a realistic range of shock angles, corresponding to conditions typically encountered in supersonic aerodynamic applications such as high-speed aircraft wings and aerofoils. This range ensures that the shock remains attached, a regime in which oblique shocks dominate, and where the Taylor-Maccoll framework remains applicable. Detached shock scenarios, which occur at larger angles or in extreme flight conditions, fall outside the intended scope of this solver.

Figure.8 compares the velocity components $u(\beta)$ and $v(\beta)$ along a conical section using the shock cone model, the conventional Taylor-Maccoll and Ishimatsu models[32]. The geometry is a 15° cone at $M_\infty = 2.0$, $\alpha = 0°$, with $\rho_\infty = 1.225$ kg/m^3. The solver's output demonstrates strong agreement with the published solutions, especially at lower shock angles. Minor deviations are observed, increasing from 2. 01% to 4. 16% with shock angle, in stronger shock conditions, reflecting the increasing complexity of tangential and normal flow resolution in those regimes.

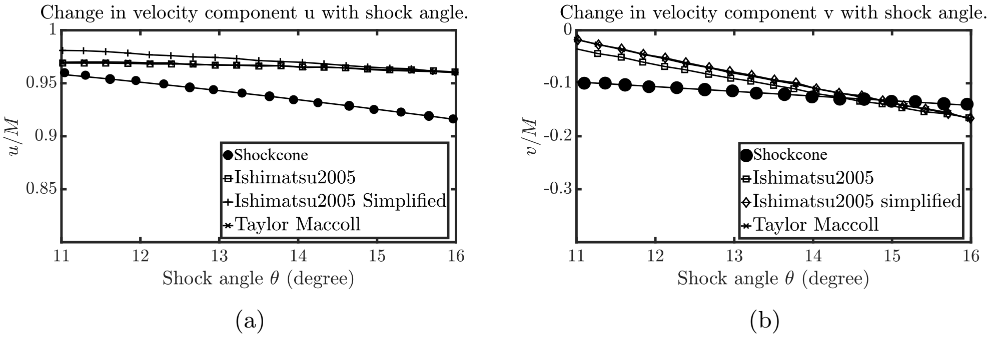

Fig. 8: Velocity component variations u(a) and v(b) with shock angle from Mach-cone influence compared with literature [32].

This validation confirms the solver's capability to replicate shockwave-related velocity changes across a practical range of configurations, supporting its integration into VLM for enhanced supersonic aerodynamic prediction. The focus on attached shock conditions ensures compatibility with linearised flow assumptions and maintains computational efficiency while significantly improving the applicability of conventional VLM in compressible flow regimes.

4.2 Results for two-dimensional shape study

This section investigates the influence of aerofoil geometry on supersonic flow behaviour using the Shockcone solver, focussing on symmetric and asymmetric two-dimensional shapes. The NACA 0012 (symmetric) and NACA 4415 (asymmetric) aerofoils were selected to assess how geometry affects shockwave interactions and drag prediction within supersonic regimes. The simulations were conducted at Mach 1.5

Boundary and Initial Conditions			
Condition	Pressure (Pa)	Temperature (K)	Velocity (m/s)
Inlet	101325	288.15	(U, 0, 0)
Outlet	*zero gradient*, 101325	*zero gradient*, 288.15	(U, 0, 0)
γ (Ratio of Specific Heat)	1.4		
Velocity (Mach)	1.5, 2.7		
Min. Allowable Wall Distance (m)	1.0×10^{-6}		
Reference Pressure (Pa)	101325		
Min. Allowable Absolute Pressure (Pa)	1000		

Table 1: Boundary and initial conditions for the simulation.

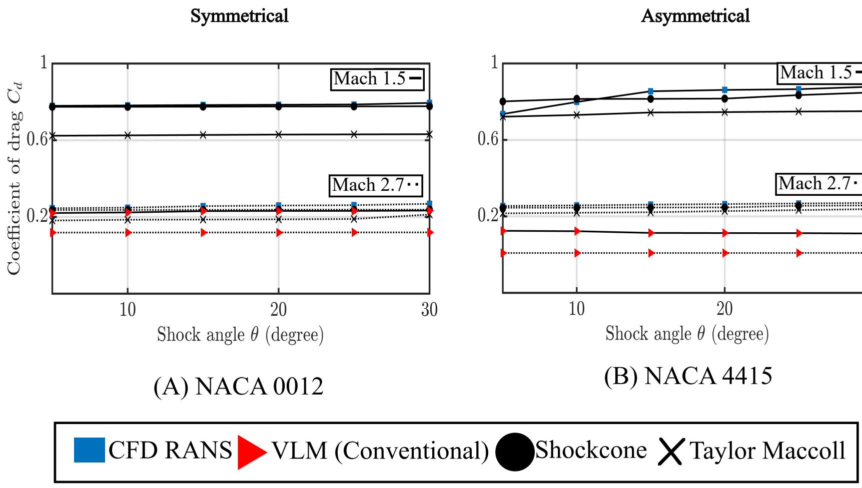

Fig. 9: Variation of pressure drag coefficient C_D with shock angle β, corresponding to increasing freestream Mach number M_∞ at constant cone angle θ_s using Shockcone solver with conventional CFD (RANS), VLM and Taylor Maccoll.

and 2.7, using consistent boundary and initial conditions derived from the literature benchmarks [37], as detailed in Table 1.

The primary aim of this shape study is to evaluate the solver's performance in capturing wave drag characteristics across varied shock angles and flow conditions. The Shockcone method—built on the integration of Taylor-Maccoll theory with the Vortex Lattice Method—offers a more physically informed approximation of conical shock interactions over lifting surfaces. This enables more accurate drag predictions compared to traditional VLM, which lacks the ability to resolve shock phenomena and surface thickness effects.

The results are summarised from running multiple simulations using different solvers such as the RANS SST, conventional VLM, Taylor-Maccoll method, and Shockcone solver. Fig 9 illustrates the Shockcone solver's results, indicating good accuracy compared to other solvers. The solid lines in the graph represent the curves from simulation running at Mach 1.5 and the dotted lines represent Mach 2.7. Fig. 9(A) shows the results for the symmetric aerofoil NACA 0012 because an aerofoil is symmetric throughout the grid providing even boundary conditions for the shockcone, which derives consistent accurate results when compared with CFD RANS. As shown in Fig. 9, the Cd predicted by the standard VLM at M = 1.5 and 2.7 deviates significantly from the CFD, particularly near the leading edge, while the VLM corrected for TMHM matches closely

This comparison reveals insights into how Taylor MacColl considers shockwave interactions over the Mach cone, capturing changes in velocity components and their influence on wave drag. In contrast, the VLM cannot account for the thickness of the surface, leading to alterations in the prediction of drag. Additionally, its inability to predict shock wave interactions and apply Mach cone influence to the lifting surface results in inaccuracies. Therefore, it can be seen from the results shown in Fig. 9 that the VLM results for Mach 1.5 and 2.7 deviate the most from that of CFD. Fig. 9 shows the consistency of the solver in predicting drag coefficients for shock angles ranging from 5 to 30 degrees.

Beyond aerodynamic accuracy, the study also highlights the solver's significant computational advantage. Compared to conventional RANS-based CFD simulations, the Shockcone solver demonstrates a drastic reduction in runtime. On average, the solver operates more than 20 times faster than the RANS CFD in all the tested cases, making it highly suitable for iterative design and early-stage aerodynamic analysis.

This computational efficiency is achieved without substantial compromise in predictive capability, particularly for practical shock angle ranges between 5° and 30°, where conical shock structures remain attached and consistent with the solver assumptions. For both types of aerofoils, the solver maintains robustness in drag prediction and provides meaningful insights into shape-induced flow variations. The integration of VLM and Taylor-Maccoll further ensures that both global and local flow characteristics are captured, offering a balanced trade-off between fidelity and speed.

In general, the two-dimensional shape study underscores the suitability of the solver for fast and reliable analysis of supersonic aerofoils. Its ability to incorporate geometric effects and resolve shock-induced flow behaviour with high computational efficiency presents a viable alternative to more resource-intensive CFD approaches, particularly in the conceptual design phase of high-speed aircraft.

4.3 Results for three-dimensional shape study

A three-dimensional shape study is crucial in aerodynamics to accurately model real-world objects and complex flow phenomena. It ensures realistic boundary conditions, validation, and reliable design exploration. Although the TMHM method originates from 2D axisymmetric theory, we extend it to 3D by applying it panel-wise based on local Mach cone alignment. In this way, we retain the simplicity of a 2D solver while enabling application to 3D geometries.

Three different supersonic configurations were considered based on the solver's assessment with wings shapes, dihedral, and swept back angles. For the following reasons, the F35 design was considered, which houses the negative dihedral from the root chord to the base chord; in addition to this The Concept supersonic design was also considered for its multiple swept-back wings on the same reference plane and to study how this configuration influences the wave drag, and lastly the Concorde configuration was used to study the solver's influence on delta wing configuration. The geometry considered was a 1:1 scale model of aircraft as in the figure 10 that was made to analyse the solver's ability to handle the full-scale model with complex mesh. The SCALOS vehicle and Concorde wing geometry information was obtained from sources and influenced by the published literature [38, 39], with simplified CAD models for surface discretization in Tornado.

The conical domain was considered to model the conical flow to accurately define the boundary condition to model the shockwave over the surface. The boundary conditions used are the same as the two-dimensional shape study with the difference in flow speeds of Mach 1 and Mach 2. For three-dimensional shape studies, the chosen shock angle range ensures accurate modelling of shock wave interactions with conical flows, which are critical in supersonic aircraft design [40].

Mesh Parameters	Selected Properties
Base Size (m)	0.75
Target Surface Size	100% of base size
Surface Growth Rate	1.1
Shock Angle (°)	10, 15, 20, 25, 30
Core Mesh Optimization Cycles	10
Quality Threshold	0.4
Number of Prism Layers	3
Volume Growth Rate	1.2

Table 2: Summary of mesh parameters and their selected properties.

Larger shock angles were not tested because they often lead to detached shocks, which requires different modelling approaches beyond the current solver's scope. This validation confirms the solver's ability to predict shockwave-induced aerodynamic effects while improving the VLM-based drag estimation.

The initialisation and boundary conditions resemble its application in studying its wave drag and its influence on the pressure drags generated by shock cone formation at supersonic speeds [41]. Fig. 11 illustrates 3D panel methods for simulating supersonic

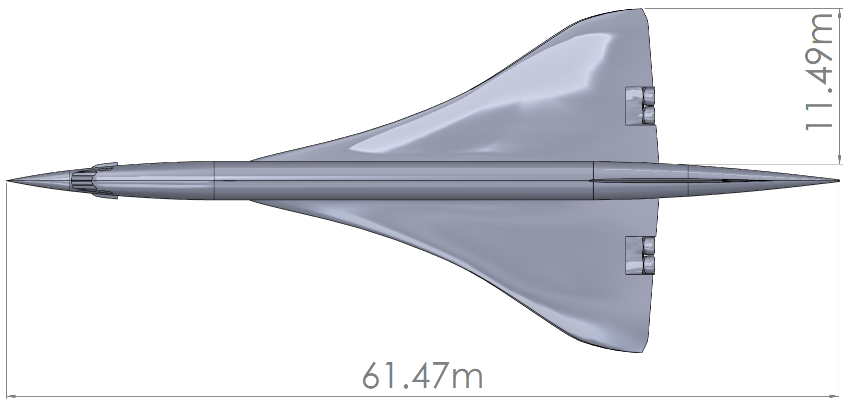

Fig. 10: Geometry for Concorde aircraft.

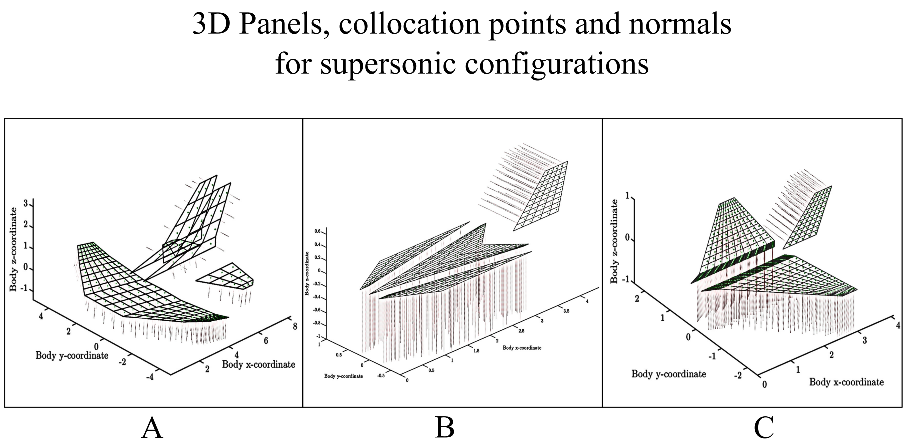

Fig. 11: Panel representation of supersonic aircraft (A) F35, (B) Concept (C) Concorde

aircraft configurations. It shows the geometries of aircraft such as (A) F35, (B) Concept (C) Concorde with their wings and tails, dissected into numerous panels along the chord and span, with the aim of mirroring the actual 3D design [42] with precision. The panels are arranged to reflect true-to-scale measurements and incorporate specific dihedral angles to match the real aircraft's geometry.
Additionally, Fig 11 highlights collocation points - critical for locating the vortex centres on each panel's surface and depicts the normal to the panels with dotted lines, which are perpendicular to the panel surfaces. To model the panels with close accuracy to the 3-D designs for the Concorde and F35 configuration the gap between the wings is left to mimic the space needed by the fuselage to generate its influence on the drag, whereas in the case of concept design that gap is filled with panels to study the effect of panels in the space on the pressure drag due to compressibility effects and wake. The panel concentration can be increased for increased accuracy of the solver, which will also increase the computational time for running the simulations.

The mesh independence study is performed as shown in the figure12 and evaluates the impact of grid refinement on the calculated drag coefficient (C_D) using the polyhedral meshing approach of STAR-CCM +. Initially, noticeable variations in C_d occur for coarser meshes, indicating numerical sensitivity to grid resolution. However, as the base mesh size is refined to 0.75m, the changes in C_d stabilise, confirming that further refinement does not significantly impact accuracy. This establishes that a base mesh size of 0.75 m is optimal, balancing computational efficiency and result precision.
These geometries are then modelled in Tornado base code to generate the lattice and defined boundary conditions. The generated geometries define the orientation of the panel, increasing concentrations on the lifting surface of the influence.

Fig 13 Showing the representation of the change in the pressure coefficient, denoted as ΔC_P, is crucial to analyse the shock wave patterns around supersonic wings. The

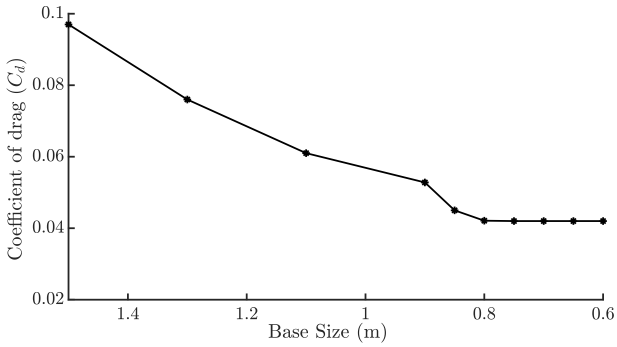

Fig. 12: Mesh independence study with coefficient of drag C_d

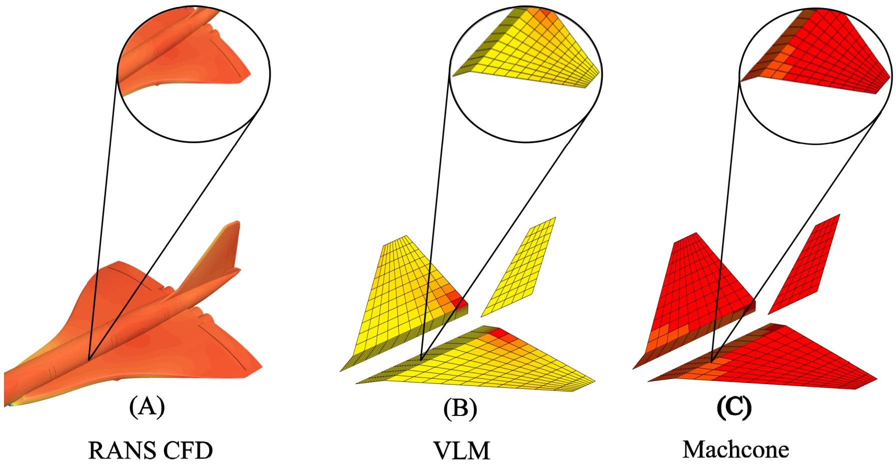

Fig. 13: Delta C_p representation over Concorde (A)RANS CFD, (B)VLM and (C)Shockcone

pressure coefficient was calculated using numerical simulations and a low-order aerodynamic model. In the numerical approach, C_P was derived from surface pressure data and the pressure difference between the lower and upper surfaces was evaluated to assess the aerodynamic loading. In the low-order method, the VLM was modified to incorporate compressibility corrections using influence coefficients derived from the Taylor-Maccoll equation, accounting for shock-expansion effects in supersonic flows. The corrected influence matrix ensured an accurate pressure distribution, allowing for a comparative assessment between the two methods.

High values of ΔC_P indicate the presence of strong shockwaves, which contribute to increased aerodynamic drag and potential instability. By examining(ΔC_P) in Fig.

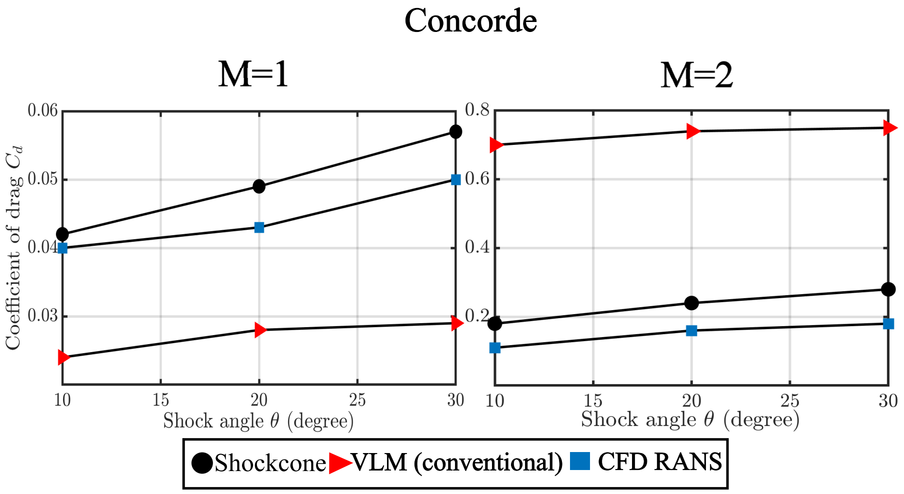

Fig. 14: Coefficient of drag comparison for concord configuration from VLM, Shockcone and RANS (CFD).

13 on the aircraft surface, areas of intense shock waves can be identified and the aircraft design can be refined to mitigate these effects. In Fig. 13 the sharp gradients in colour near the aircraft's fuselage at the quarter chord position in the images indicate the presence of a shock wave, as shown in the bubbles, which is where the airflow transitions from supersonic to subsonic speeds, causing a sudden change in air pressure and temperature [14]. The difference in shock wave angles probably affects the aerodynamic performance and drag characteristics of the aircraft. This analysis helps improve the aerodynamic efficiency of the aircraft and reduce drag by optimising the design parameters responsible for this change to mitigate the risk of wave drag in shock cone generation.
Furthermore, this information can be used carefully to understand the exact location of the shock formation and its influence on the geometry of the aircraft, such as the intricate design changes required to minimise its impact and overall improved aerodynamic performance [43]. The results are shown for the drag coefficient derived from 25 for Mach 1 and Mach 2 with shock angles of 10 to 30 degrees. The results are then compared with other solvers such as conventional VLM and RANS CFD for the same conditions. Firstly, the results for the Concorde configuration are shown to show the solver's potential over a delta-wing configuration. From Fig. 14 it seems that as the shock angle increases, the drag coefficient also increases for the Shockcone and RANS models, while the VLM model shows a relatively constant drag coefficient, which suggests that the conventional CFD does not account for the complex condition to study the surface boundary interaction at the shockcone.

Similarly for F-35 the results shown in Fig. 15 depict the VLM results are higher than the RANS and Shockcone, which was expected based on the geometry design of the configuration in VLM and its limitation with complete geometry progression when compared with conventional CFD. However, overall Shockcone shows a more

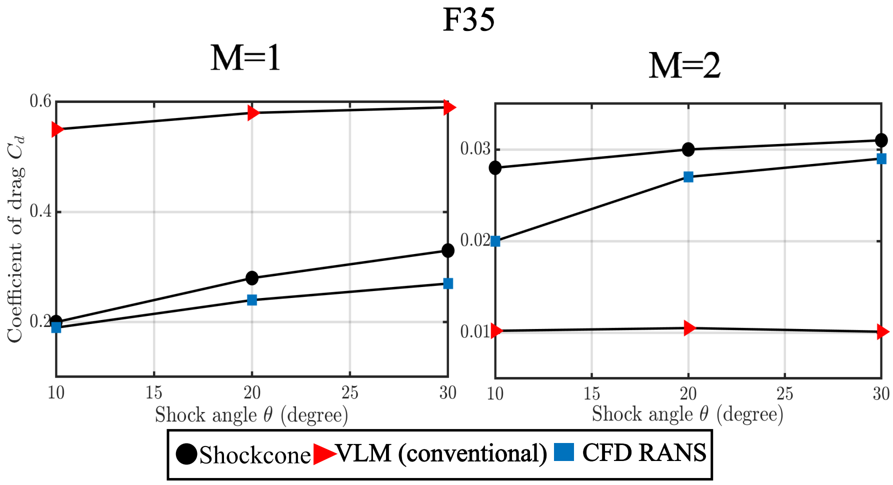

Fig. 15: Coefficient of drag comparison for F35 configuration from VLM, Shockcone and RANS (CFD).

pronounced increase, suggesting that the idealised shockwave pattern significantly impacts the drag as the angle increases. The VLM line sits above the RANS, indicating that the vortex effects captured by this method result in a higher drag prediction than the averaged turbulence model of the RANS, because of which it is verified that the conventional VLM does not account for accurate modelling of drag estimation at high speeds. The Shockcone prediction is significantly higher at larger angles, which could be due to the idealised nature of the shockwave model it represents and how it computes with a defined grid size. As has been observed from the two-dimensional shape study, the Shockcone solvers lose their accuracy with asymmetrical shapes, as it creates inconsistency in defining the boundary conditions around them concerning the grid. From the results of the last two configurations it is seen that the shock cone results in less influence on the model generating the drag, which suggests that for this configuration, the shock angle has minimal impact on drag. However, for the supersonic concept shown in Fig. 16 C_d the values are higher, with the VLM method showing a moderate increase with the shock angle and the RANS method showing a minor increase. This observation clearly states that the influence of the surface is on the shock to increase its estimated pressure drag due to compressibility effects, but it does not model viscous skin friction drag explicitly.

In all the graphs between Concorde, concept supersonic, and F35 one common thing is that the results from the Shockcone solver resonate closely with the results from the RANS CFD computations. The results converge between both for lower shock angles in the range of 10-15° whereas the shock wave increases, the results deviate from each other showing that the solver loses its consistency with increasing shock angle, which can only be proved using an experimental validation. The critical change in correlation between these results is seen after a shock angle of 20°. Overall, the results compared show potential 85% to 90% accuracy for low Mach numbers and shock angles.

The conventional VLM method remains relatively flat. This indicates that the generic configuration experiences consistent drag as the shock angle increases, particularly as expected by the VLM. Compared to others, the Shockcone method seems to be more sensitive to changes in shock angle across all configurations, suggesting a more detailed capture of the effects of shock waves on drag. This suggests that the shock cone might be the more nuanced and responsive method to capture the aerodynamic effects of shock wave angles on these aircraft configurations.

Compared to the three graphs, the RANS method consistently predicts a lower sensitivity of C_d to the shock angle, potentially indicating a more average approach to complex flow patterns, possibly missing some of the implications of shock wave behaviour [44]. The VLM and Shockcone methods show that the drag increases with shock angle, which is consistent with the physics of supersonic flow, where larger shock angles correspond to stronger shock waves and higher drag. Each graph represents different aircraft configurations, indicating how these methods might vary in their predictive capabilities based on specific aerodynamic designs.

Fig.17 shows the correlation matrix, highlighting how different parameters correlate with each other in the context of an improved Shockcone solver and conventional CFD. Each square represents the correlation coefficient between the parameters on the vertical and horizontal axes. The colour scale on the right indicates the strength of the correlation, with 1 being a perfect positive influence on the solver, indicated by a white colour square with green colour 1 written on it. Similarly, -1 is a negative influence indicated by a black square with a red -1 written on it, and 0 indicates no influence, typically shown by a neutral grey. For example, if you look at the square that intersects the "Density" row and the "Pressure" column, the colour of the square will show you how strongly those two parameters are correlated and have an influence

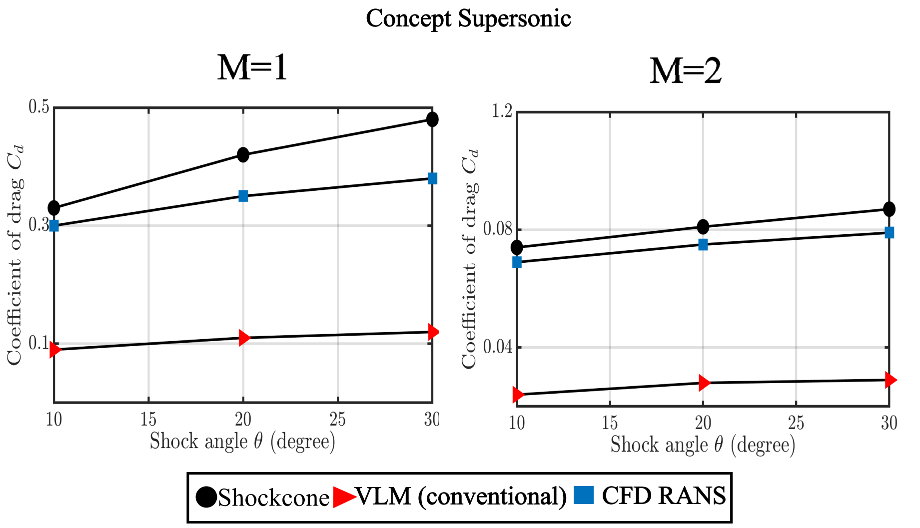

Fig. 16: Coefficient of drag comparison for concept supersonic configuration from VLM, Shockcone and RANS (CFD).

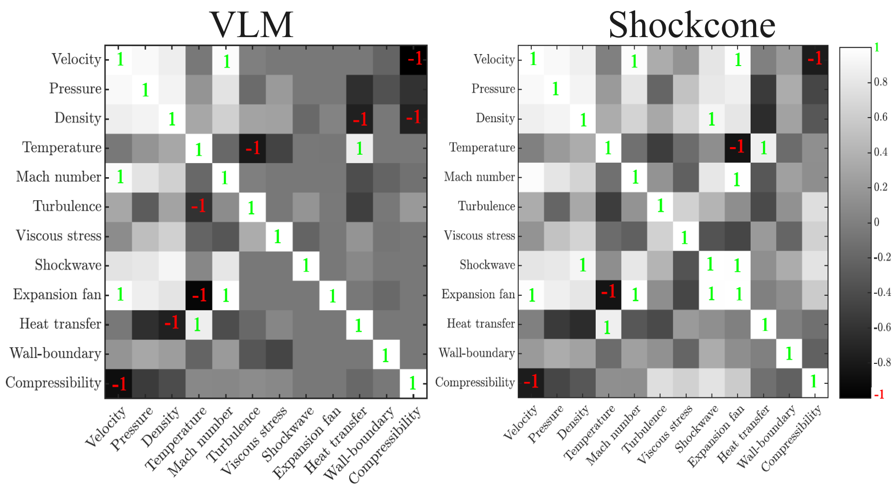

Fig. 17: Correlation box showing the relations between the improved parameters.

on the solver according to the data analysed. A bright white would mean they tend to increase and decrease together, while a black would mean that as one increases, the other tends to decrease. A neutral colour would mean there is no clear relationship between the two in the data set used, which has little to no influence on the solver. This matrix is a powerful tool for quickly assessing relationships between multiple variables in a complex system, such as the environment of shock-wave boundary interactions. In Fig. 17, the matrix on the left represents the relation between the parameters for the vortex lattice method, and on the right is the correlation matrix for the Mach cone influence. As seen from both the figures, the comparison shows that the number of green 1 signs has increased for the Shockcone solver, and similarly, the red -1 has reduced. The relation plot shows how improvements in the solver-made parameters like Viscous stress, Shockwave and expansion fan have greatly improved its influence overall, improving its capabilities to model and study the interaction of conical flows with modelling Mach cone, thereby improving the drag prediction.

5 Conclusion and Future Work

This study introduces a significant advancement to conventional VLM by integrating shock cone modelling based on the Taylor-Maccoll hypervelocity method (TMHM). This hybrid approach improves the predictive capacity of supersonic aerodynamic solvers, particularly for rapid drag estimation and shock cone interaction analysis in preliminary aircraft design. By capturing the influence of wave drag with greater fidelity, the method demonstrates up to a 20% reduction in error compared to standard VLM and achieves accuracy levels between 85% and 95% relative to high-fidelity Reynolds-average Navier-Stokes (RANS) CFD simulations.

The solver leverages potential flow theory in combination with the Taylor–Maccoll analytical framework to resolve the shockcone layer and boundary interactions over aerodynamic panels. It enables precise modelling of pressure discontinuities both upstream and downstream of the shock cone region, enhancing model validation and physical insight. The comparison results with Ishimatsu's experimental benchmarks [32] confirm the convergence behaviour at increasing cone angles, with prediction errors as low as 2.01% at shallow angles and no greater than 4. 16% at steeper angles.

Analysis of both symmetric (NACA 0012) and cambered (NACA 4415) aerofoils further demonstrates the solver's robustness across varying geometries, accurately capturing lift characteristics and lift-to-drag ratios. The precision remained consistently high, 90–95% in 2D flow simulations and 85–90% in 3D panelised configurations, highlighting the method's ability to model shock-cone-geometry interactions effectively while retaining low computational overhead.

In terms of performance, the solver operates approximately 24 times faster than traditional CFD solvers, enabling high-throughput aerodynamic analyses across a wide design envelope. This position it as an efficient and scalable tool for supersonic conceptual design, where rapid assessment across thousands of geometric variants is essential.

Future development will focus on extending the solver to capture three-dimensional shock cone structures and accommodate multiphase supersonic effects via LBM. As a mesoscopic solver, LBM offers an ideal framework for compressibility correction and shock cone-interface resolution in multiphase environments [45]. Enhancements in wall boundary conditions are also being implemented to improve accuracy in modelling viscous effects and thermal gradients in high-speed conditions [8], further expanding the solver's capability in next-generation supersonic aircraft design workflows.

References

[1] Smith, H.: A review of supersonic business jet design Issues. The Aeronautical Journal **111**(1126), 761–776 (2007) https://doi.org/10.1017/S0001924000001883

[2] Mavriplis, N., Ting, K.Y., Moustafa, A., Hill, C., Soltani, R., Nelson, C., Livne, E.: Supersonic Configurations at Low Speeds (SCALOS): Test / Simulation Correlation Studies. In: AIAA Science and Technology Forum and Exposition, AIAA SciTech Forum 2022. American Institute of Aeronautics and Astronautics Inc,, San Diego, CA, U.S.A, 3-7 January (2022). https://doi.org/10.2514/6.2022-1801 . https://arc.aiaa.org/doi/10.2514/6.2022-1801

[3] Estrada, E.G., Melin, T., Garrido Estrada, E.: Tornado supersonic module development (Master's thesis). Technical report, Linköping University (July 2010)

[4] Theerthamalai, P., Nagarathinam, M.: Aerodynamic Analysis of Grid-Fin Configurations at Supersonic Speeds. Journal of Spacecraft and Rockets **43**(4), 750–756 (2006) https://doi.org/10.2514/1.16741

[5] Joshi, H., Thomas, P.: Review of vortex lattice method for supersonic aircraft

design. The Aeronautical Journal **127**, 1–35 (2023) https://doi.org/10.1017/aer.2023.25

[6] Bliamis, C., Menelaou, C., Yakinthos, K.: Implementation of various-fidelity methods for viscous effects modeling on the design of a waverider. Aerospace Science and Technology **133**, 108141 (2023) https://doi.org/10.1016/j.ast.2023.108141

[7] Maxwell, J.R.: Efficient Design of Viscous Waveriders with CFD Verification and Off-Design Performance Analysis. In: 53rd AIAA/SAE/ASEE Joint Propulsion Conference. American Institute of Aeronautics and Astronautics, Reston, Virginia (2017). https://doi.org/10.2514/6.2017-4879

[8] Knisely, C.P., Haley, C.L., Zhong, X.: Impact of Hypersonic Boundary Layer Transition on Skin Drag and Surface Heating on Blunt Cones. In: AIAA Scitech 2019 Forum. American Institute of Aeronautics and Astronautics, Reston, Virginia (2019). https://doi.org/10.2514/6.2019-1134

[9] Wright, M.J., Sinha, K., Olejniczak, J., Candler, G.V., Magruder, T.D., Smits, A.J.: Numerical and Experimental Investigation of Double-Cone Shock Interactions. AIAA Journal **38**(12), 2268–2276 (2000) https://doi.org/10.2514/2.918

[10] Frayssinet, O.: Numerical analysis of a separated flow on a supersonic cone flare model. In: 34th AIAA Applied Aerodynamics Conference. American Institute of Aeronautics and Astronautics, Reston, Virginia (2016). https://doi.org/10.2514/6.2016-3424

[11] Martin, G.L.: Modifications to the wdtvor and vortwd computer programs for converting input data between vorlax and wave drag input formats. Technical report, NASA-CR-145360, Nasa Langley Research Center (1978)

[12] Souders, T.J., Takahashi, T.T.: Vorlax 2020: Benchmarking examples of a modernized potential flow solver. In: AIAA AVIATION 2021 FORUM. American Institute of Aeronautics and Astronautics, ??? (2021). https://doi.org/10.2514/6.2021-2459 . https://arc.aiaa.org/doi/10.2514/6.2021-2459

[13] Bowcutt, K., Kuruvila, G., Grandine, T., Cramer, E.: Advancements in Multidisciplinary Design Optimization Applied to Hypersonic Vehicles to Achieve Performance Closure. In: 15th AIAA International Space Planes and Hypersonic Systems and Technologies Conference. American Institute of Aeronautics and Astronautics, Reston, Virigina (2008). https://doi.org/10.2514/6.2008-2591

[14] Aprovitola, A., Dyblenko, O., Pezzella, G., Viviani, A.: Aerodynamic Analysis of a Supersonic Transport Aircraft at Low and High Speed Flow Conditions. Aerospace **9**(8), 411 (2022) https://doi.org/10.3390/aerospace9080411

[15] Sandlin, D.R., Pessin, D.N.: Aerodynamic analysis of hypersonic waverider

aircraft NASA-CR-192981. Technical report, California Polytechnic State University, California (April 1993)

[16] Kinney, D.: Aero-Thermodynamics for Conceptual Design. In: 42nd AIAA Aerospace Sciences Meeting and Exhibit. American Institute of Aeronautics and Astronautics, Reston, Virigina (2004). https://doi.org/10.2514/6.2004-31

[17] Shi, A., Chen, J., Dowell, E.H., Wen, H.: Approach to Determine the Most Efficient Supersonic Mach Number. AIAA Journal **58**(3), 1402–1406 (2020) https://doi.org/10.2514/1.J058773

[18] Taylor, G.I., Maccoll, J.W.: The A ir Pressure on a Cone Moving at High Speeds.-II. Technical report (1931). https://royalsocietypublishing.org/

[19] Taylor, G.I., Maccoll, J.W.: The Air Pressure on a Cone Moving at High Speeds. I on JSTOR. In: Proceedings of the Royal Society of London, pp. 278–297. Royal Society, London (1933). https://www.jstor.org/stable/95973

[20] Brooks, G.P.: Verification and Validation for Pseudospectral Shock Fitted Simulations of Supersonic Flow Over a Blunt Body. AIAA Aerospace Sciences Meeting and Exhibit **42**(1), 1–13 (2004)

[21] Ueno, A., Suzuki, K.: CFD-Based Shape Optimization of Hypersonic Vehicles Considering Transonic Aerodynamic Performance. In: 46th AIAA Aerospace Sciences Meeting and Exhibit. American Institute of Aeronautics and Astronautics, Reston, Virigina (2008). https://doi.org/10.2514/6.2008-288

[22] Hu, S., Qu, S., Zheng, Z., Zhu, P., Zou, C., Li, Y.: Investigation of aerodynamics education based on the waverider parameterized design procedure. Thermal Science **27**(2 Part B), 1393–1404 (2023) https://doi.org/10.2298/TSCI220311032H

[23] Loewenthal, E., Gopalarathnam, A.: Low-Order Modeling of Wingtip Vortices in a Vortex Lattice Method. AIAA Journal **60**(3), 1708–1720 (2022) https://doi.org/10.2514/1.J060654

[24] Kontogiannis, A., Laurendeau, E.: Adjoint State of Nonlinear Vortex-Lattice Method for Aerodynamic Design and Control. AIAA Journal **59**(4), 1184–1195 (2021) https://doi.org/10.2514/1.J059796

[25] Musa, O., Huang, G., Jin, B., Mölder, S., Yu, Z.: New Parent Flowfield for Streamline-Traced Intakes. AIAA Journal **61**(7), 2906–2921 (2023) https://doi.org/10.2514/1.J062744

[26] Musa, O., Huang, G., Yu, Z.: Evaluation of the Pressure-Corrected Osculating Axisymmetric Flows Method for Designing Hypersonic Wavecatcher Intakes with Shape Transition. Journal of Aerospace Engineering **37**(3) (2024) https://doi.org/10.1061/JAEEEZ.ASENG-5241

[27] Drayna, T., Nompelis, I., Candler, G.: Hypersonic Inward Turning Inlets: Design and Optimization. In: 44th AIAA Aerospace Sciences Meeting and Exhibit. American Institute of Aeronautics and Astronautics, Reston, Virigina (2006). https://doi.org/10.2514/6.2006-297

[28] Shahriar, A., Kumar, R., Shoele, K.: Vortex dynamics of axisymmetric cones at high angles of attack. Theoretical and Computational Fluid Dynamics **37**(3), 337–356 (2023) https://doi.org/10.1007/s00162-023-00647-0

[29] XIANG, G., WANG, C., TENG, H., JIANG, Z.: Shock/shock interactions between bodies and wings. Chinese Journal of Aeronautics **31**(2), 255–261 (2018) https://doi.org/10.1016/j.cja.2017.11.012

[30] Guillermo-Monedero, D., Whitfield, C.A., Freuler, R.J., Mccrink, M.H.: A Comparison of Euler Finite Volume and Supersonic Vortex Lattice Methods Used During the Conceptual Design Phase of Supersonic Delta Wings (Master's Thesis). Ohio State University, Columbus, U.S.A (2020)

[31] Settles, G.S., Dodson, L.J.: Supersonic and hypersonic shock/boundary-layer interaction database. AIAA Journal **32**(7), 1377–1383 (1994) https://doi.org/10.2514/3.12205

[32] Ishimatsu, T., Morishita, E.: Taylor-Maccoll Hypervelocity Analytical Solutions. The Japan society for aeronautical and space sciences **48**(159), 46–48 (2005) https://doi.org/10.2322/tjsass.48.46

[33] Schobeiri, M.T.: Compressible Flow. In: Advanced Fluid Mechanics and Heat Transfer for Engineers and Scientists, pp. 447–496. Springer, Cham (2022). https://doi.org/10.1007/978-3-030-72925-7_13

[34] Roohi, E., Stefanov, S., Shoja-Sani, A., Ejraei, H.: A generalized form of the Bernoulli Trial collision scheme in DSMC: Derivation and evaluation. Journal of Computational Physics **354**, 476–492 (2018) https://doi.org/10.1016/j.jcp.2017.10.033

[35] Melin, T.: User's Guide and Reference Manual for Tornado. vol. 1, 2.3 edn., pp. 1–45. Royal Institute of Technology KTH, Stockholm (2000)

[36] PACK, D.C.: A note on Prandtl's formula for the wave-length of a supersonic gas jet. The Quarterly Journal of Mechanics and Applied Mathematics **3**(2), 173–181 (1950) https://doi.org/10.1093/qjmam/3.2.173

[37] Lorenzon, D.: Open FOAM simulations of the supersonic flow around cones at angles of attack. Journal of Mechanical and Civil Engineering **16**(5), 67–79 (2019)

[38] Orlebar, C.: Concorde vol. 1, pp. 27–65. Bloomsbury Publishing, ??? (2017)

[39] Nelson, C.P., Ting, K.-Y., Mavriplis, N., Soltani, R., Livne, E.: Supersonic configurations at low speeds (scalos): Project background and progress at university of washington. In: AIAA SCITECH 2022 Forum. American Institute of Aeronautics and Astronautics, ??? (2022). https://doi.org/10.2514/6.2022-1803

[40] Munday, D., Gutmark, E., Liu, J., Kailasanath, K.: Flow structure and acoustics of supersonic jets from conical convergent-divergent nozzles. Physics of Fluids **23**(11) (2011) https://doi.org/10.1063/1.3657824

[41] Sun, Y., Smith, H.: Low-boom low-drag solutions through the evaluation of different supersonic business jet concepts. The Aeronautical Journal **124**(1271), 76–95 (2020) https://doi.org/10.1017/aer.2019.131

[42] Jones, T.: NASA's Quiet Supersonic Aircraft. Technical report, Oshkosh, WI (July 2017)

[43] Nangia, R., Ghoreyshi, M., Rooij, M.P.C., Cummings, R.M.: Aerodynamic design assessment and comparisons of the MULDICON UCAV concept. Aerospace Science and Technology **93**, 105321 (2019) https://doi.org/10.1016/j.ast.2019.105321

[44] Coburn, N.: Compressible Supersonic Flow in Jets under the Kármán-Tsien Pressure-Volume Relation. Journal of Applied Physics **22**(2), 124–130 (1951) https://doi.org/10.1063/1.1699912

[45] Renard, F., Feng, Y., Boussuge, J.-F., Sagaut, P.: Improved compressible hybrid lattice Boltzmann method on standard lattice for subsonic and supersonic flows. Computers & Fluids **219**, 104867 (2021) https://doi.org/10.1016/j.compfluid.2021.104867